Bioorganic & Medicinal Chemistry 21 (2013) 766–778

Contents lists available at SciVerse ScienceDirect

Bioorganic & Medicinal Chemistry

journal homepage: www.elsevier.com/locate/bmc

The discovery of novel isoflavone pan peroxisome proliferator-activated receptor agonists

Azadeh Matin [a], Munikumar Reddy Doddareddy [a], Navnath Gavande [a], Srinivas Nammi [b,†], Paul W. Groundwater [a], Rebecca H. Roubin [a], David E. Hibbs [a,*]

[a] Faculty of Pharmacy, The University of Sydney, Sydney, NSW 2006, Australia
[b] School of Science and Health, University of Western Sydney, Locked Bag 1797, Penrith, NSW 2751, Australia

ARTICLE INFO

Article history:
Received 29 August 2012
Revised 11 November 2012
Accepted 17 November 2012
Available online 3 December 2012

Keywords:
PPARα
PPARγ
PPARδ
Pan PPAR agonist
Type II diabetes mellitus
Metabolic syndrome
Peroxisome proliferator-activated receptor

ABSTRACT

Twenty three dual PPARα and γ molecules of natural product origin, previously reported by our group, were further investigated for pan PPAR transactivation against PPARδ. The in vitro cell toxicity profile, as well as, in silico study of the most active molecules within this new class of pan PPAR agonists are also described. 3′,5′ Dimethoxy-7 hydroxyisoflavone **6**, Ψ-baptigenin **7**, 4′ fluoro-7 hydroxyisoflavone **8**, and 3′ methoxy-7 hydroxyisoflavone **9** were identified as the most potent molecules studied within the set compared to the commercially available pan PPAR agonist, bezafibrate **1**. These novel active molecules may thus be useful as future leads in PPAR-related disorders, including type II diabetes mellitus and metabolic syndrome.

1. Introduction

The PPAR family consists of three subtypes, namely PPAR alpha, PPAR gamma and PPAR delta/beta that are encoded by three distinct genes.[1–5] Each isotype exhibits different patterns of tissue distribution, has specific pharmacological activators, ligand specificity, and physiological roles.[1,2,4,6]

PPAR alpha is mainly found in tissues with a high rate of fatty acid metabolism, including: brown adipose tissue, liver, kidney, heart and muscle.[1,3,5] It plays an important role in the inflammatory response, uptake and oxidation of fatty acids and lipoprotein metabolism, as well as glucose homeostasis.[1,4] Unsaturated fatty acids, leukotriene B4, and 8 hydroxyeicosatetraenoic acid are endogenous ligands of PPAR alpha.[5,7]

PPAR gamma is principally expressed in adipose tissue, intestinal cells, and macrophages, in addition to being localized at lower concentrations in other tissues including skeletal muscle and endothelium.[1] This receptor is involved in the regulation of adipocyte proliferation and differentiation, as well as glucose homeostasis and insulin sensitization.[1] Unsaturated fatty acids, 15-hydroxyeicosatetraenoic acid, 9- and 13-hydroxyocta-decadienoic acid and 15-deoxyΔ12,[1] prostaglandin J2 have been reported as PPAR gamma endogenous ligands.[7,5] However, they have shown to bind PPAR gamma at micromolar levels, therefore indicating that it may not be the case.[8]

PPAR delta is localized more ubiquitously and is found in most cell types.[1] Numerous studies have highlighted the physiological importance of PPAR delta in the regulation of fatty acid catabolism, energy homeostasis, wound healing, blastocyst implantation, as well as lipid trafficking in macrophages and trophoblasts.[9,10] PPAR delta endogenous ligands are unsaturated fatty acids, carbaprostacyclin and components of very low density lipoproteins.[7]

It has been suggested that pan peroxisome proliferator-activated receptor (PPAR) agonists which have the ability to activate all three PPAR isoforms (α, γ, and δ)[11,12] may have advantages over PPARγ and dual PPARα and γ agonists in the treatment of metabolic disorders such as type 2 diabetes mellitus (T2DM) and cardiovascular disease. Such pan PPAR agonists might overcome some of the limitations associated with current PPAR drugs, which include weight gain and cardiovascular risks.[11–22] Recent studies have highlighted the cardioprotective role of PPARδ, as well as its potential in targeting dyslipidemia and the alleviation of weight gain.[15,23–26] The stimulation of PPARδ complements the role of PPARα in treating lipid abnormalities, in addition to helping to prevent the weight gain that is a typical adverse effect of PPARγ agents.[15,23,27–29]

* Corresponding author. Tel.: +61 2 93516005; fax: +61 2 93514391.
E-mail address: david.hibbs@sydney.edu.au (D.E. Hibbs).
† Current address.

0968-0896/$ - see front matter © 2012 Elsevier Ltd. All rights reserved.
http://dx.doi.org/10.1016/j.bmc.2012.11.040

Bezafibrate **1** is a pan PPAR agonist that has been on the market for more than 25 years. It has a good safety profile but relatively low potency (Fig. 1).[11,15,21,30,31] Several pan PPAR agonists with enhance activity, such as netoglitazone (PGX-510 or MCC-555) **2**[11,13,14,31] and DRL 11605,[11,32] are either currently being evaluated or are at early stages of clinical trials, although the therapeutic potential for these new classes of drugs remain uncertain. The development of some pan PPAR agonists including, sipoglitazar (TAK-654) **3**, GW-625019, sodelglitazar (GW-677954) **4** and indeglitazar (PPM-204 or PLX-204) **5**, has been terminated due to toxicity concerns (Fig. 1).[11,32–34] The development of novel and efficacious pan PPAR agonists with improved safety profiles is thus of great interest.

In our previous paper,[35] we investigated five classes of flavonoids (flavanones, flavones, isoflavones, chalcones, and their pyrazole derivatives) for dual PPARα and γ activity. In total 75 compounds were examined, with 23 showing dual activity, and four of the isoflavones **6**, **7**, **8**, and **9** being identified as the most potent dual PPARα and γ agonists (Fig. 2). In this Letter, we present our extended study on the 23 dual PPARα and γ agonists[35] and report on their activation of PPARδ, and hence, pan agonist activity. In addition, we describe the cytotoxicity profile and in silico docking results obtained for the most efficacious pan PPAR agonists identified in this work.

2. Results and discussion

2.1. PPARδ biological evaluation

The 23 dual PPARα and γ agonists reported in our previous paper,[35] which included flavanones, flavones and isoflavones, were further investigated for pan PPAR agonist activity against PPARδ. The compounds were examined for in vitro PPARδ transactivation[36] in the human embryonic kidney (HEK) 293 cell line, with the commercially available pan PPAR agonist bezafibrate, which is known to have a slightly higher preference for PPARδ over the other PPAR isoforms,[5] used as a reference. All 23 compounds were evaluated at both 25 and 40 μM as bezafibrate is known to provide optimal activation at these concentrations.[35] Dimethyl sulfoxide (DMSO) solution (0.1% v/v) acted as the vehicle control. The minimal PPARδ fold activation obtained with the vehicle control was considered to be one-fold activation and the results are summarized in Table 1. Of these 23 compounds evaluated for PPARδ transactivation activity, only compound **12** has been investigated for this purpose.[37]

The flavanones (**15**–**16**) were weak agonists; at 25 and 40 μM, compound **15** (1.1- and 1.3-fold activation, respectively) and compound **16** (1.2- and 1.3-fold activation, respectively) exhibited only slight PPARδ activity compared to bezafibrate (7.5- and 12.0-fold activation, respectively).

In the flavone series, compound **22** (1.1- and 1.2-fold PPARδ activation at 25 and 40 μM, respectively) was the least active molecule within the set. The other flavones **17**–**21** and **23**–**28** were also weakly active (2.3- to 4.2-fold activation at 25 μM, 4.2- to 7.3-fold activation at 40 μM), and showed much lower activity than bezafibrate at the same concentrations (7.5- and 12.0-fold activation, respectively).

Of the isoflavones evaluated, compounds **10** (1.1- and 1.9-fold activation at 25 and 40 μM, respectively) and **14** (1.7- and 2.3-fold activation, respectively) demonstrated the lowest activity at the concentrations tested but compound **11** (7.4- and 12.2-fold activation, respectively) exhibited similar potency to bezafibrate (7.5- and 12.0-fold activation, respectively), while compounds **12** (6.7- and 11.0-fold activation, respectively) and **13** (6.5- and

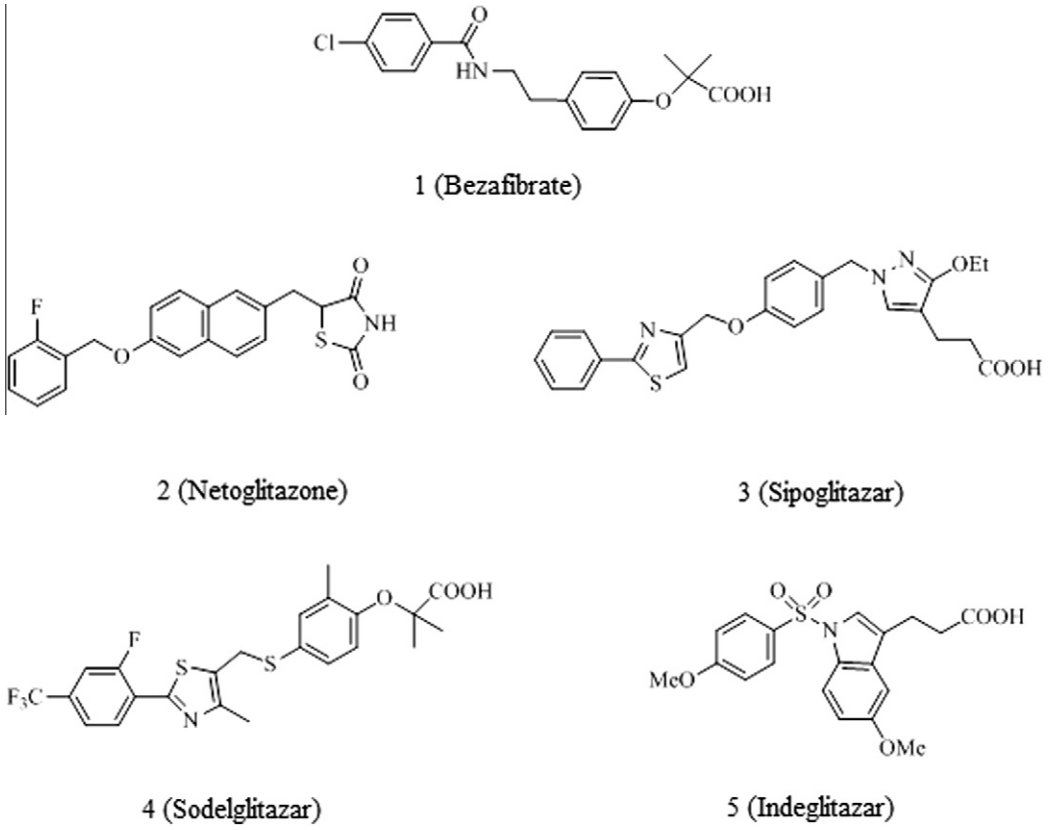

Figure 1. Chemical structures of some pan PPARα, γ and δ agonists.[1,2]

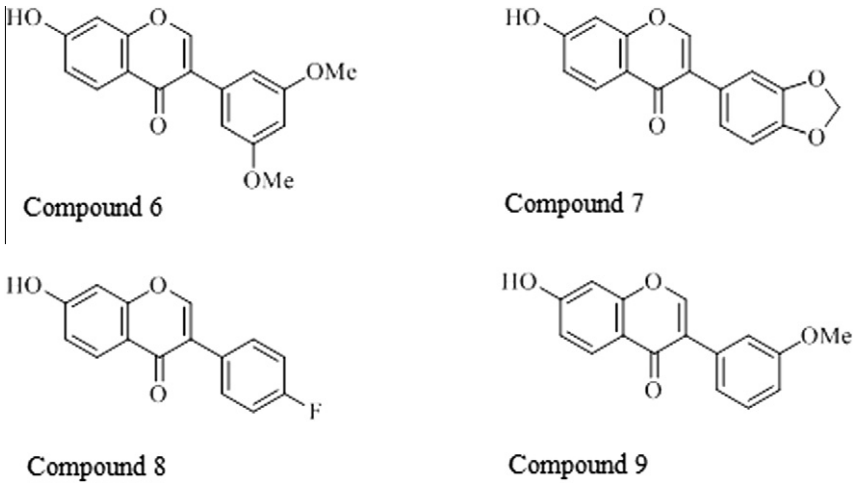

Figure 2. Chemical structures of the most active dual PPARα and γ molecules reported in our previous paper.[35]

Table 1
In vitro PPARδ activation by 23 dual PPARα and γ agonists

Compounds	PPARδ fold activation (SEM)[a]	
	25 μM	40 μM
1 Bezafibrate	7.5 (0.59)	12.0 (1.5)
6 (3′,5′-Dimethoxy-7-hydroxyisoflavone)	17.5 (1.6)	34.9 (2.3)
7 (Ψ-baptigenin)	12.2 (1.1)	24.4 (2.2)
8 (4′-Fluoro-7-hydroxyisoflavone)	12.0 (0.9)	14.2 (1.6)
9 (3′-Methoxy-7-hydroxyisoflavone)	54.8 (2.8)	109.2 (3.5)
10 (3′,4′-Methylenedioxy-7-(tetrahydropyran-2-yloxy)isoflavone)	1.1 (0.08)	1.9 (0.18)
11 (4′-Methoxy-7-hydroxyisoflavone)	7.4 (0.78)	12.2 (0.95)
12 (Daidzein)	6.7 (0.51)	11.0 (1.2)
13 (4′,6,7,-Trihydroxyisoflavone)	6.5 (0.53)	10.4 (0.98)
14 (7-Methoxy-ψ-baptigenin)	1.7 (0.14)	2.3 (0.19)
15 (Naringenin)	1.1 (0.14)	1.3 (0.10)
16 (Hesperetin)	1.2 (0.11)	1.3 (0.15)
17 (7,2′-Dihydroxyflavone)	2.9 (0.34)	4.8 (0.53)
18 (7,3′-Dihydroxyflavone)	3.3 (0.27)	5.1 (0.48)
19 (7,4′-Dihydroxyflavone)	3.5 (0.41)	5.9 (0.40)
20 (6,4′-Dihydroxyflavone)	2.7 (0.31)	4.7 (0.36)
21 (5,4′-Dihydroxyflavone)	2.3 (0.24)	4.2 (0.34)
22 (3′,4′-Dihydroxyflavone)	1.1 (0.12)	1.2 (0.15)
23 (Apigenin)	3.9 (0.48)	6.3 (0.57)
24 (Acacetin)	3.4 (0.25)	6.0 (0.45)
25 (Chrysoeriol)	3.9 (0.32)	6.5 (0.52)
26 (Diosmetin)	4.1 (0.37)	7.1 (0.54)
27 (Chrysin)	2.5 (0.29)	4.5 (0.35)
28 (Kaempferol)	4.2 (0.35)	7.3 (0.58)

[a] Fold activation compared to vehicle control, where the mean relative luciferase activity was normalized to the β-galactosidase activity of two experiments performed in triplicate.

10.4-fold activation, respectively) showed slightly reduced activity. The PPARδ activation by compound **12** was different to that reported PPARδ activity by Dang et al.[37] and this is most likely due to the different transactivation methods and cell lines used.

The highest PPARδ agonist activity in the isoflavone series was observed for compounds **6** (17.5- and 34.9-fold activation at 25 and 40 μM, respectively), **7** (12.2- and 24.4-fold activation, respectively), **8** (12.0- and 14.2-fold activation, respectively), and **9** (54.8- and 109.2-fold activation, respectively) (Fig. 3). It is noteworthy that these very active PPARδ agonists were the most active dual PPARα and PPARγ agonists reported in our previous paper.[35]

2.2. EC_{50} study

The PPARδ EC_{50} profiles of the most potent pan PPAR isoflavones **6**, **7**, **8**, and **9** were compared to that of bezafibrate at six different drug concentrations (0, 0.1, 3, 10, 30, and 100 μM). The dose–response curves are shown in Figure 4 and the EC50 values summarized in Table 2. To provide a better insight into the pan PPAR activity of these molecules, the PPARγ and PPARα EC_{50} values[35] are also included in Table 2.

As can be seen from Table 2, isoflavones **6**, **7**, **8**, and **9** (EC_{50} = 17.17, 22.34, 24.39, and 12.44 μM, respectively) are almost twice as potent activators of PPARδ than bezafibrate (EC_{50} = 35.74 μM). Compound **9**, with an EC_{50} of 12.44 μM, produced the greatest PPARδ activation. The EC_{50} of bezafibrate was slightly different to that previously reported EC_{50},[5] presumably as a result of the different transactivation methods and cell lines used. In addition, the EC_{50} value for rosiglitazone is different to that reported in the literature.[5] This is most likely due to the different transactivation plasmid systems used in the assay, e.g., full-length hPPARγ and tk-PPREx4-Luc plasmids used in our assays (EC_{50} in

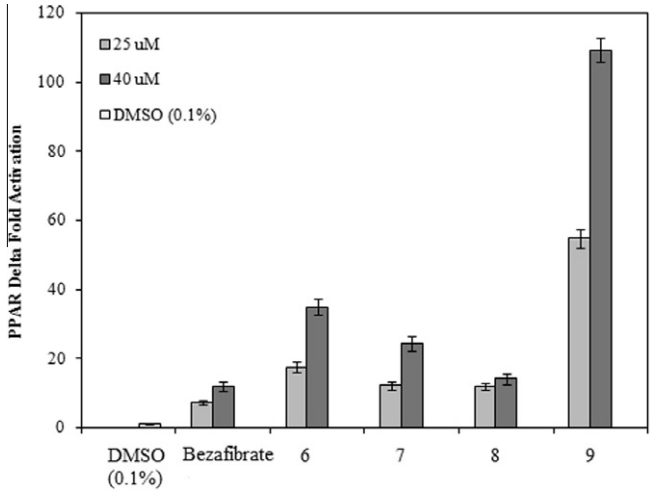

Figure 3. PPARδ luciferase reporter transactivation of the most efficacious isoflavone derivatives (25 and 40 μM) compared to the positive control bezafibrate. All values are expressed as fold activation compared to DMSO vehicle control, where the relative luciferase activity is normalized to the β-galactosidase signal, mean ± SEM of two experiments performed in triplicate.

the μM range[38]) versus chimeric fusion protein GAL4-PPARγ-LBD and GAL4-Luc plasmids (EC_{50} in the nM range). The transactivation plasmids used in our assay correspond more closely to the actual in vivo cellular transactivation.[35]

Comparison of the PPARδ EC_{50} values with the corresponding PPARα and γ EC_{50} data (Table 2) highlights the differences in selectivity of these agonists towards each of the PPAR isoforms. Compound **9** produced the weakest PPARα (EC_{50} = 33.13 μM) and PPARδ (EC_{50} = 12.44 μM) activation, while compound **8** was the strongest PPARγ agonist (EC_{50} = 15.38 μM).

Compound **6** showed similar efficacy for PPARγ (EC_{50} = 18.86 μM) and PPARδ (EC_{50} = 17.17 μM) and a lower activation of PPARα (EC_{50} = 24.55 μM). In contrast, compound **7** produced weaker PPARγ activation (EC_{50} = 26.94 μM) than a PPARδ (EC_{50} = 22.34 μM) or PPARα (EC_{50} = 8.9 μM) activation. Compound **8** demonstrated greater activation of PPARγ (EC_{50} = 15.38 μM) and similar activation of PPARα (EC_{50} = 23.10 μM) and PPARδ (EC_{50} = 24.39 μM). Compound **9** was a more potent agonist of PPARδ (EC_{50} = 12.44 μM) compared to PPARγ (EC_{50} = 22.29 μM) and PPARα (EC_{50} = 33.13 μM). Each of these four pan PPAR agonists were thus found to be unique in their preferences and selectivity for PPARα, γ, and δ isoforms.

2.3. SAR study

The lower PPARδ activity observed for the flavanones (**15–16**) suggests that the planar structure of the flavones and isoflavones is a requirement for PPARδ activation. The data for the flavone and the isoflavone families highlights the vital role of the 7-OH group for the activation of PPARδ. Compounds **22** (flavone), **10,** and **14** (isoflavones), which were the only three agonists within the set that lacked the 7-OH moiety all exhibited insignificant PPARδ agonism, in contrast to the compounds evaluated.

The isoflavones led to greater PPARδ activation than the flavones, indicating the importance of the phenyl ring on the C-3 position of the chromane skeleton, rather than the C-2 position. In addition, the introduction of alkoxy/halogen substituents at the

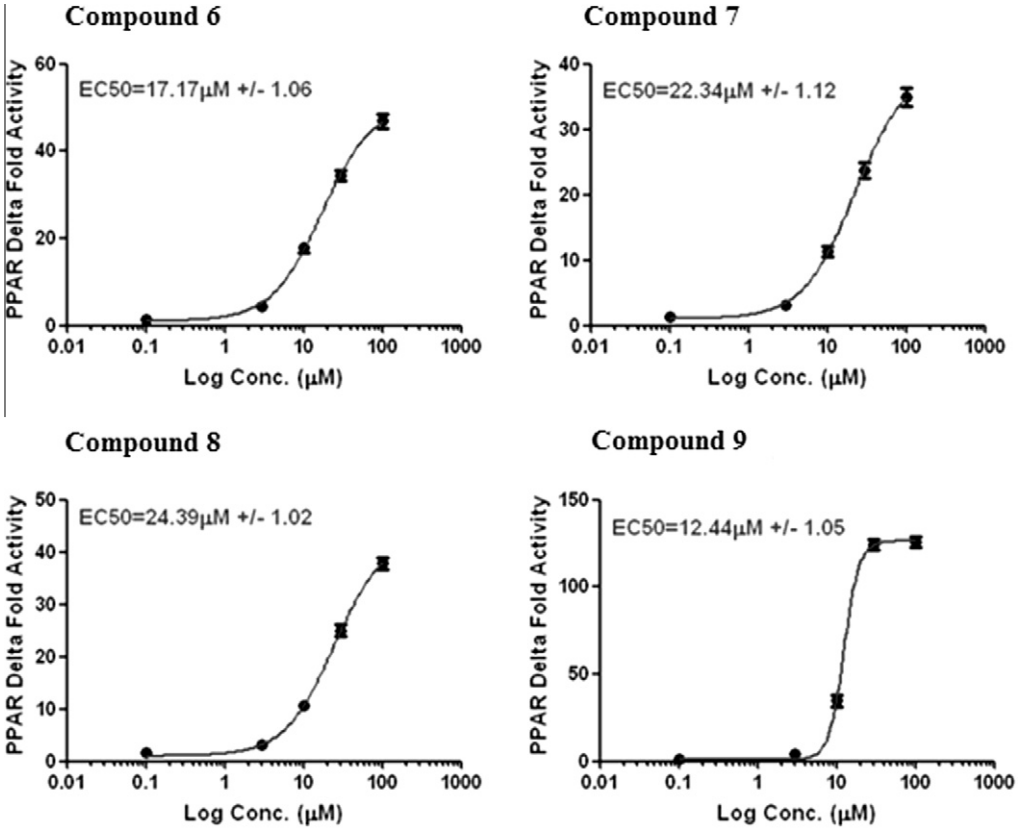

Figure 4. PPARδ dose response curves of the top 4 PPAR active compounds (**6**, **7**, **8**, and **9**, respectively) calculated using the Prism Software (log drug concentration in μM vs PPARδ fold activation). EC_{50} values for PPARδ agonist activity were calculated as the concentration of the test ligand (μM) required for the half-maximal fold induction of luciferase activity. Data shown are means ± SEM from three experiments performed in triplicate.

Table 2
The in vitro transactivation activity profile (EC_{50}) of the most active pan PPARα, γ, and δ agonists

Compounds	Transactivation EC_{50} (μM, SEM)[a]			Selectivity
	hPPARα[25]	hPPARγ[25]	hPPARδ	
Bezafibrate	46.58 (1.10)	70.36 (1.04)	35.74 (1.15)	hPPARδ > hPPARα > hPPARγ
Fenofibrate	33.51 (1.02)	—	—	hPPARα
WY-14643	23.33 (1.07)	—	—	hPPARα
Rosiglitazone	—	43.71 (1.08)	—	hPPARγ
6	24.55 (1.06)	18.86 (1.04)	17.17 (1.06)	hPPARγ = hPPARδ > hPPARα
7	8.90 (1.10)	26.94 (1.08)	22.34 (1.12)	hPPARα > hPPARδ > hPPARγ
8	23.10 (1.04)	15.38 (1.02)	24.39 (1.02)	hPPARγ > hPPARα = hPPARδ
9	33.13 (1.05)	22.29 (1.05)	12.44 (1.05)	hPPARδ > hPPARγ > hPPARα

[a] EC_{50} values for PPARα, γ, and δ agonist activity were calculated as the concentration of the test compound (μM) required for the half-maximal fold activation of luciferase activity. Data shown are means (SEM) from three experiments conducted in triplicate.

3, 4, and 5 positions of the isoflavone B ring resulted in significantly higher PPARδ activity, with the substituent position determining the activity. Methoxy substitution at the 3 and 3,5 positions of the B ring was found to lead to greater activation that at the 4 position; compounds **9** (3′-methoxy) and **6** (3′,5′-dimethoxy) elicited a greater PPARδ activation than compound **11** (4′-methoxy). Isoflavones **6** (3′,5′-dimethoxy), **7** (3′,4′-methylenedioxy), **8** (4′-fluoro), and **9** (3′-methoxy) demonstrated substantially higher PPARδ agonist activity compared to the other agonists evaluated, with compound **9** (3′-methoxy) being identified as the most potent PPARδ agonist.

2.4. Cytotoxicity profile of the pan PPAR isoflavones

In order to investigate whether the top four pan PPAR agonists (**6**, **7**, **8**, and **9**) were toxic, we used the HEK293 cell line as an in-vitro cytotoxicity model, with cytotoxicity profiles established at various concentrations (0–100 μM) using the CellTiter 96 Aqueous One Solution cell proliferation assay, with bezafibrate as the positive control and DMSO solution (0.1% v/v) as the vehicle control.

As illustrated in Figure 5, treatment with compounds **7** and **9** resulted in greater than 90% cell viability at 10 μM, while compounds **6** and **8** produced cell viabilities of 80% and 78%, respectively, and were thus found to be less toxic than bezafibrate (76%) at the same concentration. Compound **9** was the only agonist that resulted a cell viability of 74% at 100 μM, and this is comparable to bezafibrate (73.7%). In summary, the isoflavones **6**, **7**, **8**, and **9** demonstrated greater cell viability (>78%) than bezafibrate (76%) at 10 μM concentration and therefore were found to be less toxic than bezafibrate at lower concentrations. Compound **9** was identified as the least cytotoxic agonist evaluated within the set. The cell viability values we obtained for bezafibrate indicate slightly greater toxicity than that previously reported in the literature.[39,40] These differences are probably due to the previous cell viability studies being conducted in a different in vitro cytotoxicity model, a human embryonal rhabdomyosarcoma (HRMSC) cancer cell line, using different cell proliferation assays (WST-8 and WST-1).

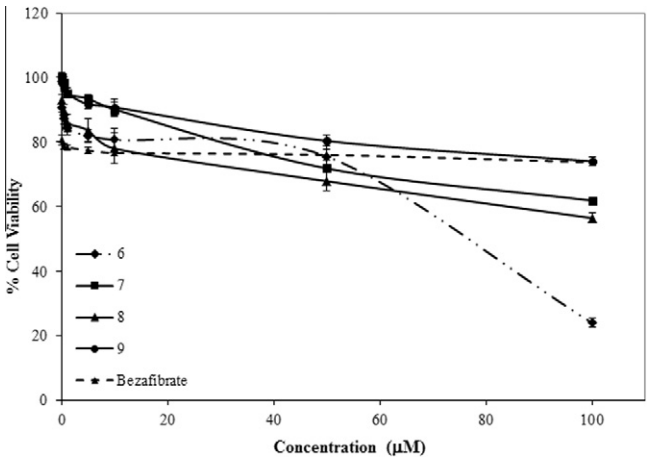

Figure 5. Cytotoxicity profiles of compounds **6**, **7**, **8**, **9**, and PPAR pan agonist bezafibrate. Cell viability was determined using the MTS Assay. The results are expressed as % relative cell viability compared to DMSO vehicle control. All values are mean ± SEM of two experiments performed in quadruplicate.

2.5. Molecular modeling of the most potent pan PPAR isoflavones

The top four pan PPAR agonists were further investigated by in silico docking studies using Glide (Maestro[41]) in order to provide an insight into the binding interactions between the four active agonists and the three PPAR isoforms and so suggest an explanation for their differing potencies towards each PPAR subtype. The binding behavior of these four compounds was also investigated through comparison with that of known full[42] and partial[43] PPARγ agonists in order to establish their mode of action.

2.5.1. Binding interactions with PPARγ

A typical PPARγ agonist usually has a polar head group (capable of hydrogen bonding), as well as a hydrophobic tail for interactions within the Y shaped PPARγ ligand binding cavity (Arm I, Arm II and the entrance).[1] The isoflavones identified in this study contain a hydroxyl substituent on their chromane moiety and also a hydrophobic B ring that allows them to make these pivotal interactions with the PPARγ. Compounds **6**, **7**, **8**, and **9** were docked in to a PPARγ crystal structure (PDB ID: 2Q59, resolution: 2.2 Å)[43] using the extra precision (XP) mode of Glide application, and their binding interactions with the receptor investigated.

In the docking experiments we utilized the crystal structure of PPARγ bound to ligand MRL20 (PDB ID: 2Q59) and the binding pose of MRL20 was successfully re-created in the docking process, with a root mean square deviation (RMSD) value of 0.037 Å. As illustrated in Figure 6, all the docked compounds fitted the active site in a similar orientation and all exhibited two hydrogen bonds between their polar moieties and the PPARγ. The 7-OH substituent of the compounds forms a hydrogen bond with Glu295 (H3 helix); while the polar oxygen of their pyranone ring affords the second hydrogen bond with the Glu343 residue (loop connecting the S3 and S4 β strands) of the receptor.

The docking results reveal that the B ring of the isoflavones is located in a cavity that consists of many hydrophobic amino acid residues, including Cys285, Ile281, Val339, Ile341, Met348, Leu353 and Met364. Compound **8**, which results in the greatest PPARγ activation (EC_{50} = 15.38 μM), contains a hydrophobic fluoro

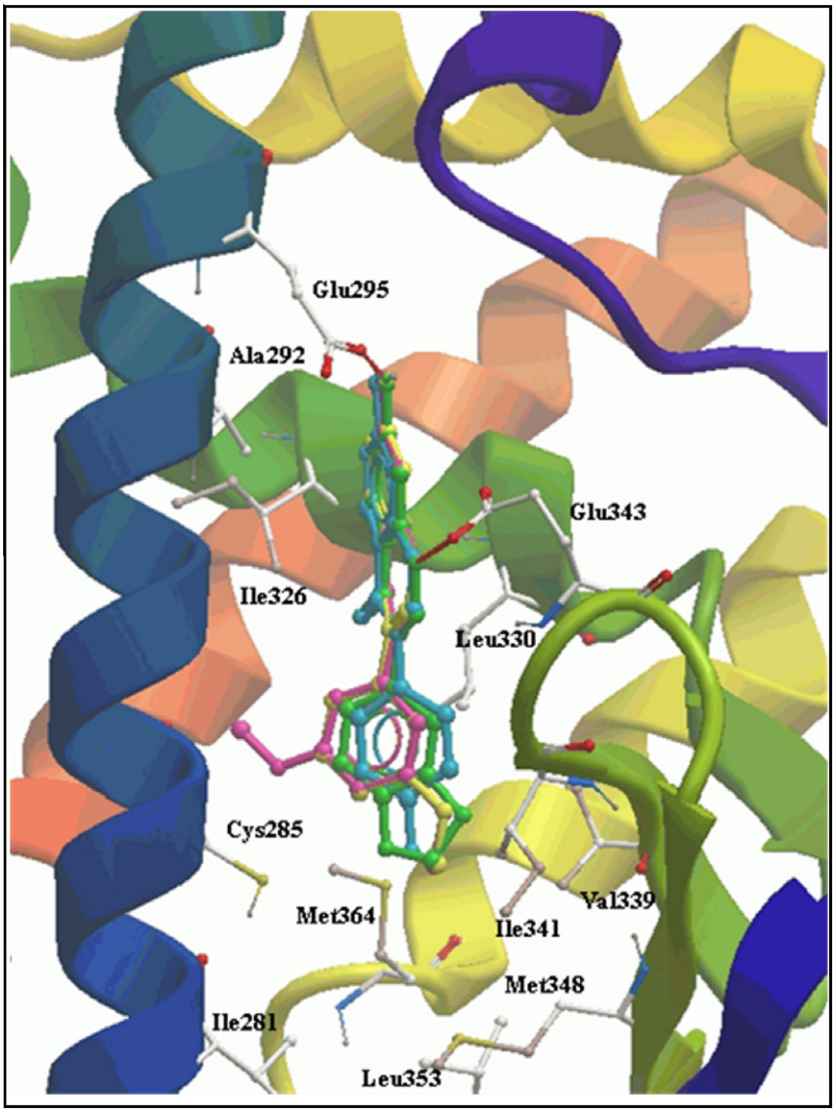

Figure 6. The top four active compounds docked in the ligand binding domain of PPARγ protein crystal structure (PDB ID: 2Q59). Compounds **6**, **7**, **8**, and **9** are depicted in magenta, green, cyan, and yellow colours, respectively. The image was created using ICM software.

substituent on the 4 position of the B ring and binds well in this cavity. Compound **6** (EC_{50} = 18.86 μM), the second most active ligand, has a dimethoxy substituent with the two methoxy groups interacting with the hydrophobic pocket in a favourable manner. In contrast, compound **9** contains only one methoxy substituent and therefore has fewer interactions with the receptor, resulting in a slight decrease in activity (EC_{50} = 22.29 μM). Compound **7**, with the lowest PPARγ activation (EC_{50} = 26.94 μM) of the four compounds, bears a hydrophilic 3′,4′-methylenedioxy moiety in the hydrophobic cavity leading to a further decrease in activity.

All the compounds can thus form two hydrogen bonds with the amino acid residues, Glu295 and Glu343 of the PPARγ ligand binding domain (LBD), through their 7-OH substituent and the polar oxygen of their pyranone ring, respectively. Compound **8** (4′-fluoro) exhibited the most favourable interactions with the hydrophobic pocket of the receptor and had the greatest activity.

2.5.2. Binding interactions with PPARα

Compounds **6**, **7**, **8**, and **9** were docked into the PPARα crystal structure (PDB ID: 1K7L, resolution: 2.5 Å).[44] 1K7L is the crystal structure of PPARα bound to ligand GW409544. This in silico study aimed to investigate the different potencies observed for the agonists against PPARα (EC_{50} = 24.55, 8.90, 23.10 and 33.13 μM, respectively). The accuracy of the docking process was examined by docking the ligand, GW409544, into the 1K7L crystal structure; the docked GW409544 successfully recreated its original crystallographic binding pose with RMSD value of 0.019 Å.

As shown in Figure 7, all the docked compounds fitted the receptor in the same orientation as each other and formed two hydrogen bonds with the PPARα in the active site. The 7-OH substituent of the isoflavones forms a hydrogen bond with Glu286 amino acid (H3 helix); while the polar oxygen of the pyranone carbonyl group forms the second hydrogen bond with the Tyr334 residue (loop connecting the S3 and S4 β strands) of the receptor.

It is noteworthy that, as documented by Zoete et al.,[1] almost 80% of the amino acid residues which constitute the PPAR LBD are conserved across the three PPAR isotypes (α, γ, and δ) and the differences can be correlated with ligand specificity. The sequence alignment of the three PPAR isotypes shows that Glu286 and Tyr334 residues of the PPARα protein are at the same position as Glu295 and Glu343 of the PPARγ protein (Fig. 8), suggesting that these agonists bind at the same position in both PPAR isoforms.

Compound **9**, with the lowest PPARα activation (EC_{50} = 33.13 μM), has a methoxy substituent on the 3 position of the

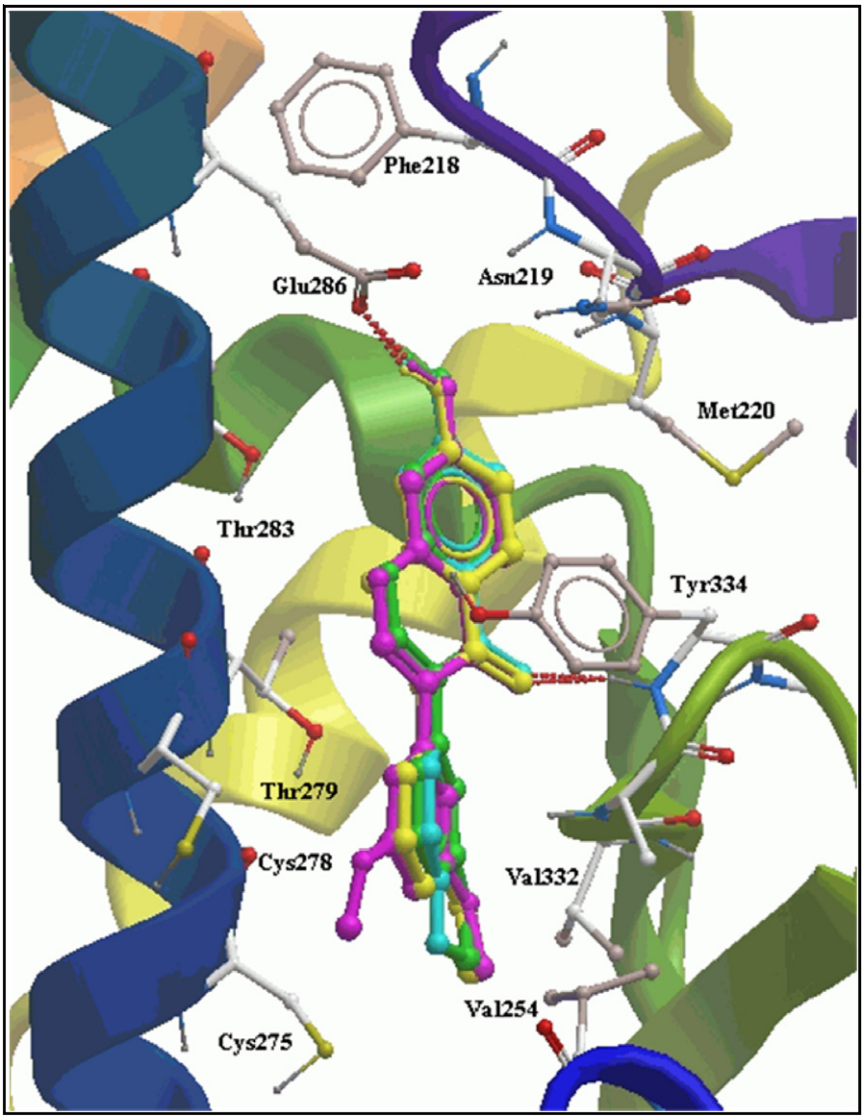

Figure 7. The top four active compounds docked in the LBD of PPARα protein crystal structure (PDB ID: 1K7L). Compounds **6**, **7**, **8**, and **9** are depicted in magenta, green, cyan, and yellow colours, respectively. The image was created using ICM software.

B ring and the hydrophobic methyl moiety of this group is situated in an area of the LBD surrounded by hydrophobic residues, with Val254, Val332, Cys275 and Cys278 making the most favourable interactions, especially the hydrophobic sulphur moieties of Cys275 and Cys278 which are orientated directly towards this methyl group. In addition, the hydrophilic oxygen of the methoxy substituent was found to have suboptimal interactions with the hydrophilic oxygens of the carboxylate moiety of Cys275 (Fig. 7), resulting in the lower potency of compound **9**. Compound **8**, containing a hydrophobic fluoro group at the 4 position of the B ring, and compound **6**, with 3′,5′-dimethoxy substitution, showed similar activities (EC_{50} = 23.10 μM and 24.55 μM), whereas compound **7**, with a hydrophilic 3′,4′-methylenedioxy substituent, showed the highest PPARα activity (EC_{50} = 8.9 μM) of the four compounds, as was observed in PPARγ study.

All four compounds can thus form two hydrogen bonds with Glu286 and Tyr334 of the PPARα LBD through their 7-OH substituent and the polar oxygen of their pyranone carbonyl group. Compound **7** (3′,4′-methylenedioxy), which had the highest PPARα activity, exhibited the most favourable interactions with the hydrophilic section of the binding pocket. It is interesting to observe that the compounds docked into the PPARα crystal structure bound in the same space, and showed a similar hydrogen bonding network to that observed in the PPARγ in silico study. Compound **8**, however, was found to have the highest PPARγ activity, while compound **9** had the highest PPARα activity, and we suggest that this difference in potency is due to the differences in the LBD amino acid composition (approx. 20%) between the two receptors.

2.5.3. Binding interactions with PPARδ

The binding interaction of the pan PPAR agonists with the active site residues of PPARδ was also investigated in silico. For this study the active isoflavones were docked into 2Q5G PPARδ crystal structure (resolution: 2.7 Å)[45] co-crystallized with 1FA ligand. Once again, the native ligand IFA was employed in the study as a measure of docking accuracy, which optimally superimposed its original crystallographic pose with an RMSD value of 0.026 Å.

The isoflavones docked in the 2Q5G PPARδ crystal structure (Fig. 9) all showed a similar binding pose and this is consistent with the observed docking poses in the PPARγ and PPARα in silico studies. All four compounds, however, could form only one

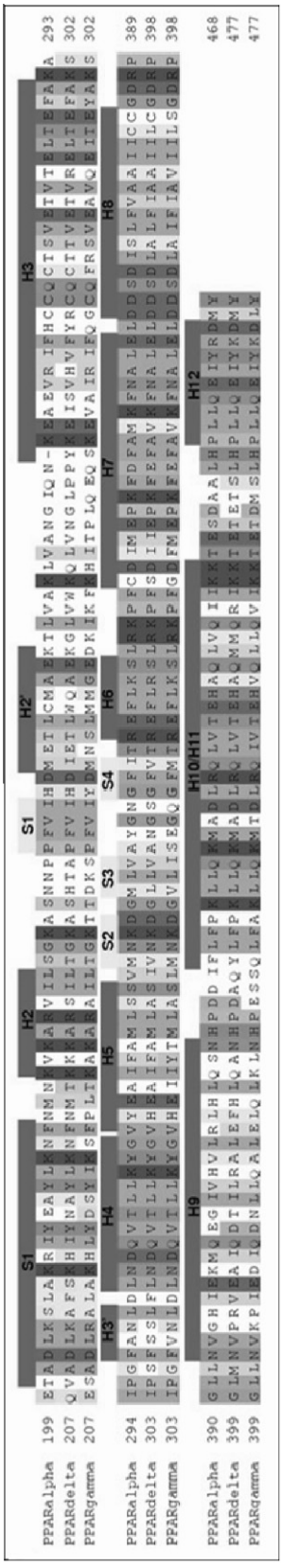

Figure 8. The sequence alignment of the LBD of the three PPAR isotypes (α, γ, and δ) reported by Zoete et al.[34] used in our study as a reference.

hydrogen bond between the 7-OH substituent of the isoflavones and Thr292 amino acid (H3 helix) of PPARδ (Fig. 9), in contrast to the hydrogen bonding network observed in the PPARγ and PPARα studies, where two hydrogen bonds were formed.

Compound **9**, the most potent PPARδ ligand studied within the set (EC_{50} = 12.44 μM), contains a methoxy substituent on the 3′ position of the B ring, which is accommodated well in the hydrophobic pocket of the LBD surrounded by hydrophobic amino acid residues such as Phe282, Cys285, Leu339, Ile363 and Ile364 (Fig. 9). In addition, this pocket also contains two basic amino acids (Lys367 and His449) which form cation–π interactions with the B ring. The other three compounds also contain substituents which are nicely accommodated within the hydrophobic cavity, leading to activities ranging from 17.17 to 24.39 μM.

Interestingly, all four compounds docked in PPARδ in a space slightly below that observed in the PPARα and γ crystal structures, and did not interact with Glu286 and Glu295 amino acid residues as seen in PPARα and γ studies, respectively; forming a hydrogen bond with Thr292. This is believed to be due to differences in amino acid composition, as well as slight topological variations between the PPARδ LBD (which is narrower in some parts) and the other two receptors.

2.5.4. Binding behaviour study of the isoflavones (full vs partial)

There are two groups of PPARγ agonists, best known as full agonists and partial agonists/specific PPAR modulators (SPPARMs). The full agonists make a distinct interaction with the Tyr473 (helix 12/AF2 domain/Arm I) of the LBD of the PPARγ thereby antagonizing the receptor. The full agonists stabilize helix 12 of the LBD, while the partial agonists/SPPARMs activate the receptor through stabilization and interactions with other parts of the protein LBD, including the entrance of the binding cavity and the β sheet.[1,11,12]

The binding interaction of the active isoflavones was compared to both full and partial PPAR agonists in order to establish their mode of action. For this study, three different PPARγ crystal structures were employed (PDB ID: 1FM6,[42] 2Q59[43] and 2Q5S[43]). The first two crystal structures represent the PPARγ bound with the full agonists, rosiglitazone and MRL20, while in the latter; the receptor was co-crystallized with the partial agonist nTZDpa.

Compounds **6**, **7**, **8**, and **9** were docked into all the three PPARγ crystal structures along with rosiglitazone, MRL20, and nTZDpa as controls for each respective receptor. As illustrated in Figure 10A–C, in contrast to rosiglitazone and MRL20 (full agonists), the isoflavones did not interact with Tyr473 of helix 12. The docked compounds posed in the vicinity of the β sheet in a similar manner to nTZDpa (partial agonist). Thus, it was concluded that although these active isoflavones exert a much higher transactivation activity than the known full PPARγ agonists (e.g. rosiglitazone), they do not interact with Tyr473 of helix 12 of the LBD, which is necessary for full agonist behaviour. Instead they interact mostly in the vicinity of the β sheet in a similar manner to partial agonists/ SPPARMs; thus highlighting the unique binding of these novel isoflavones.

2.6. Preliminary in vivo studies of isoflavone 9

The genetically defective pre-diabetic Zucker diabetic fatty (ZDF) rats are characterized by obesity, hyperphagia and insulin resistance. They develop glucose intolerance by 10 weeks of age, which progressively deteriorates as they get older (15 weeks old) and are hence typically considered to be optimum models for pre-diabetic in vivo studies.[46] The anti-diabetic efficacy of pan PPAR ligand **9** with the lowest cytotoxicity profile and the highest selectivity for PPAR alpha and delta isotypes was evaluated in vivo on 9 weeks old pre-diabetic male ZDF rats for of 6 weeks.

Healthy Zucker lean (ZL) rats of the same age were also used in the study as controls. The rats were divided into four groups as shown in Table 3. Group 1 (ZDF) and group 2 (ZL) were treated in the evenings with 3 mg/kg/day of potential diabetic drug

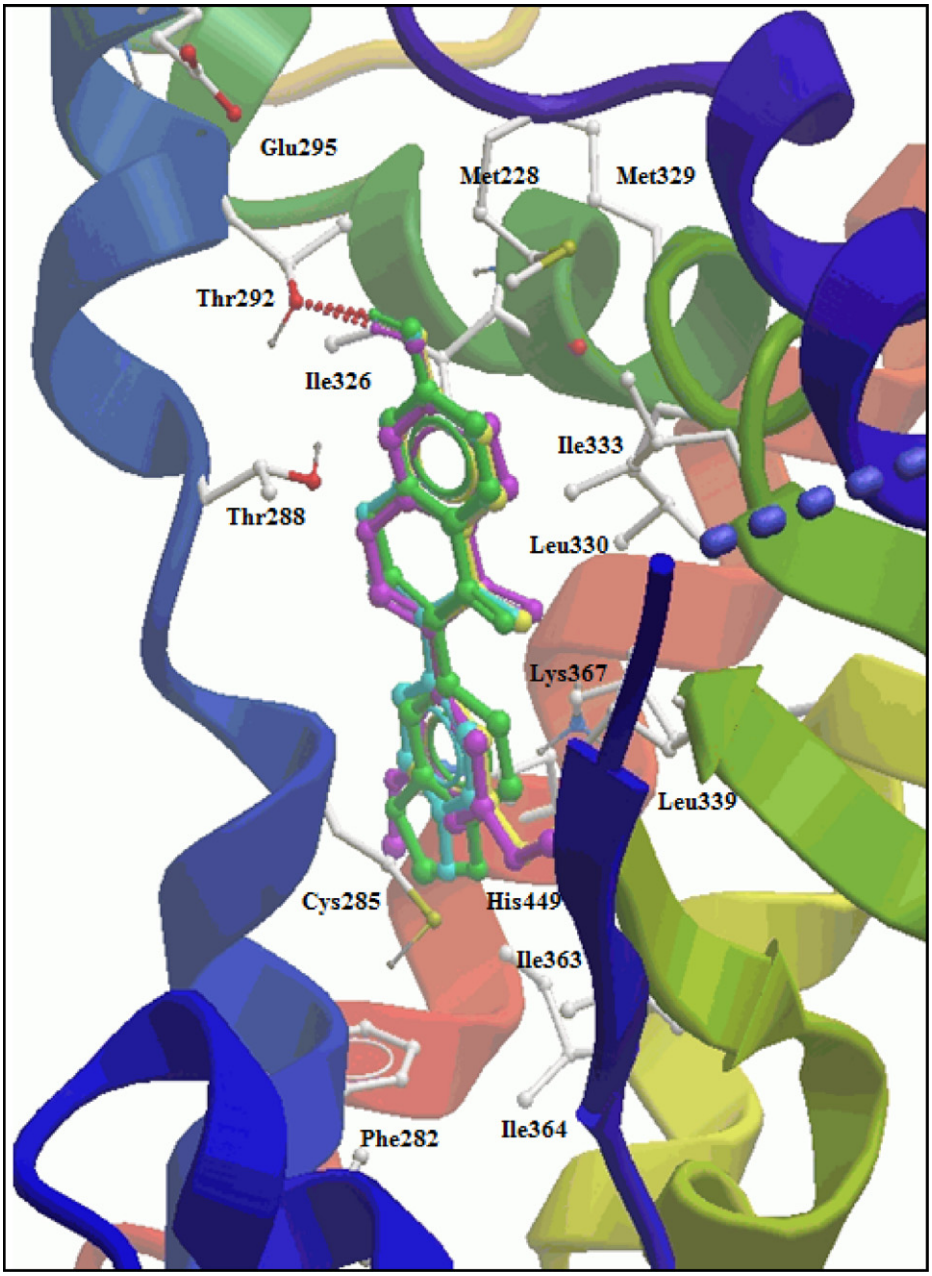

Figure 9. The top four active compounds docked in the LBD of PPARδ protein crystal structure (PDB ID: 2Q5G). Compounds **6**, **7**, **8**, and **9** are depicted in magenta, green, cyan, and yellow colours, respectively. The image was created using ICM software.

compound **9**, while group 3 (ZDF) and 4 (ZL) were exposed only to the acacia solution (controls). Animals were housed in groups of 3–4 per cage and fed with standard pelleted diet and water. In total, 14 rats were used in this preliminary study.

Obesity is one of the main factors influencing insulin resistance in T2DM and weight loss will ameliorate insulin sensitivity and increases the glucose metabolism.[47] In our in vivo study, the body weight gain of the rats was monitored every evening before the drug treatment and the feeding process, while the food intake was measured every morning. The acquired body weight gain of the four animal groups collected over the 6 weeks of the study is presented in Figure 11. As expected, the ZL rats afforded a lower body weight gain compared to the ZDF rats (63 g vs 103 g, week 6, untreated animals). Interestingly in week three of the study, the drug treated ZDF rats started to demonstrate reduced body weight gain compared to the control untreated ZDF rats. The resulting weight gain reduction was statistically significant in week six of the study (94 g vs 103 g, p <0.05). The results obtained clearly elucidate alleviation of weight gain induced by compound **9** in the ZDF drug treated rats. This beneficial effect is envisaged to be due to PPAR alpha and delta agonism activity of the novel pan PPAR ligand.

Oral glucose tolerance test is a routine medical procedure used with the diabetic patients. It measures body's ability to maintain blood glucose homeostasis upon glucose induced hyperglycemia.[48] In week 5 of the study, the animals were fasted overnight and subjected to an oral glucose tolerance test. In brief, a blood sample was taken from the animals and their blood glucose content at the fasted state determined, after which 2 g/kg of glucose solution was administered to the rats and blood samples collected at 15, 30, 45, 60, 90 and 120 min after the oral glucose intake.

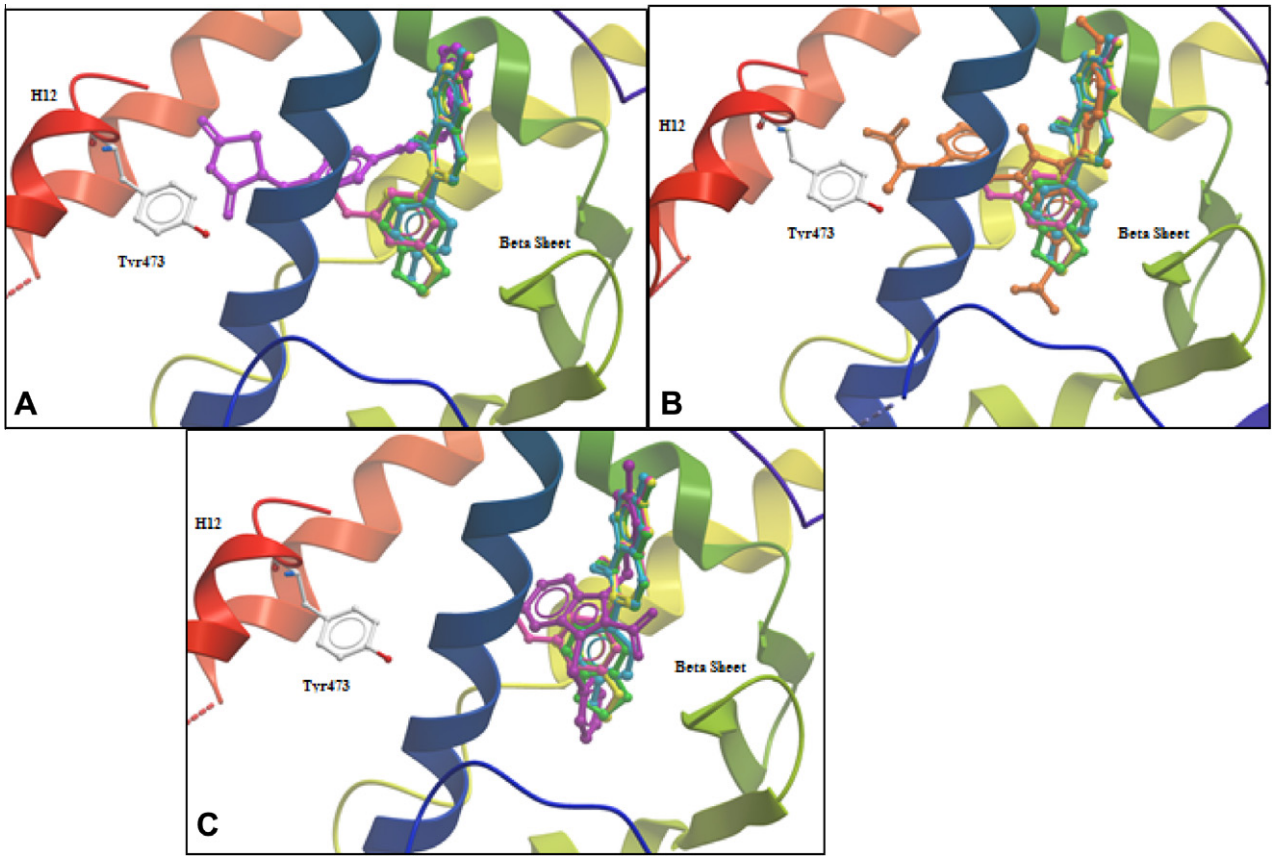

Figure 10. (A) Compounds **6** (magenta), **7** (green), **8** (cyan), **9** (yellow), and rosiglitazone (purple) docked in the ligand binding domain of the PPARγ protein (PDB ID: 1FM6). Rosiglitazone interacted with Tyr473, however, the isoflavones did not interact with this amino acid. (B) The four active compounds and MRL20 (orange) docked in the LBD of the PPARγ protein (PDB ID: 2Q59). MRL20 interacted with Tyr473. The isoflavones, however, did not interact with this amino acid. (C) The four active compounds and nTZDpa (purple) docked in the LBD of the PPARγ protein (PDB ID: 2Q5S). The isoflavones fitted the receptor in the vicinity of the β sheet, consistent with nTZDpa. No interaction with Tyr473 was observed. All the images were created using ICM software.

Table 3
The four different animal groups studied in vivo

Groups	Animals	Treatment	No. animals
1	ZDF	Drug treated	3
2	ZL	Drug treated	4
3	ZDF	Acacia treated (control)	4
4	ZL	Acacia treated (control)	3

The obtained blood glucose content acquired over the 2 h period of the study is illustrated in Figure 12. The ZL drug treated and control rats reacted in a similar manner to the glucose tolerance test and demonstrated 95–98 (mg/dL) blood glucose level at the fasted state and 120–124 (mg/dL) blood glucose level after 2 h of the glucose intake. The data obtained was in agreement with the reported blood glucose levels for healthy individuals by the U.S. National Institute of Health (NIH) at zero minute (<110 mg/dL) and at 2 h (<140 mg/dL)[49] time intervals of the glucose tolerance test.

The ZDF rats treated with compound **9** showed a slightly lower blood glucose content (113 mg/dL) than the control untreated ZDF rats (124 mg/dL) prior to the glucose administration at zero minutes. In addition, they exhibited a lower glucose peak (247 mg/dL) at 30 min compared to the ZDF control group (270 mg/dL). More interestingly, the drug treated pre-diabetic animals afforded a lower blood glucose level after 2 h of the glucose intake (154 mg/dL) than the untreated pre-diabetic rats (185 mg/dL). The obtained blood glucose data for the control ZDF rats correlated well with the upper level of the pre-diabetes profile, while the acquired data for the drug treated ZDF rats were more agreeable with the lower level of the borderline pre-diabetes profile reported by the U.S. NIH

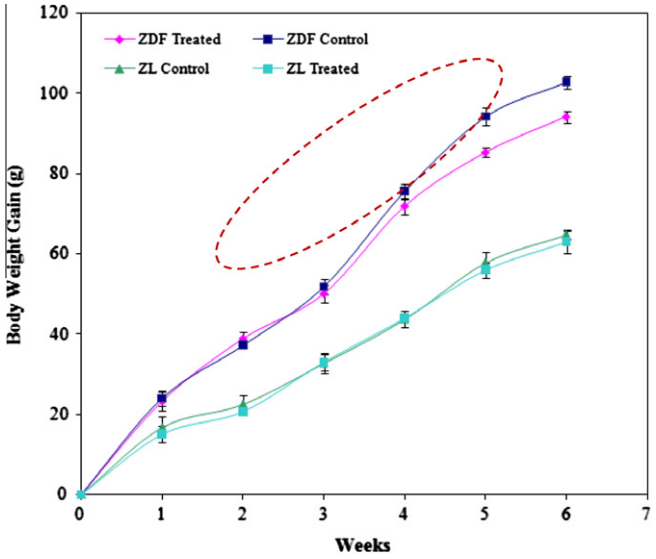

Figure 11. Body weight gain profile of the four animal groups over the course of study. ZDF drug treated ($n = 3$), ZDF control ($n = 4$), ZL drug treated ($n = 4$), ZL control ($n = 3$). The presented values are mean ± SEM.

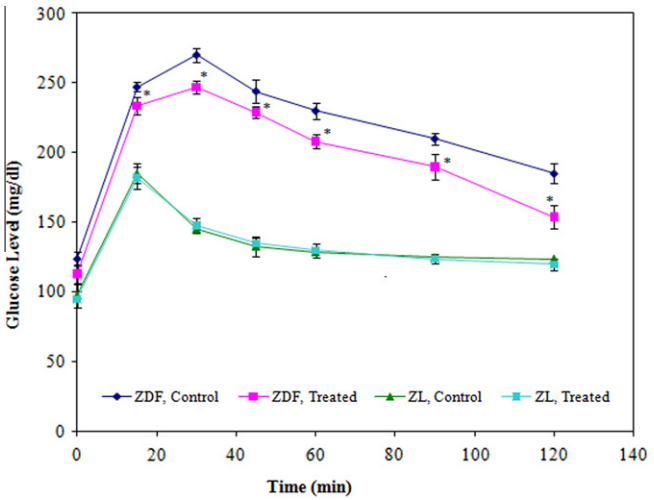

Figure 12. The glucose tolerance profile of the four animal groups studied. ZDF drug treated ($n = 3$), ZDF control ($n = 4$), ZL drug treated ($n = 4$), ZL control ($n = 3$). The presented values are mean ± SEM. $^{*}p$ <0.05 compared to ZDF control.

(110 mg/dL < 0 min < 126 mg/dL and 140 mg/dL < 2 h < 200 mg/dL).[49] Moreover, the demonstrated blood glucose content by the control untreated ZDF rats after 2 h of the glucose intake corresponded well with the studies of Augstein et al.[50]

The optimum results obtained from the pre-diabetic ZDF treated rats with the pan PPAR ligand **9** compared to the untreated pre-diabetic ZDF rats highlighted the improved glucose lowering efficacy of this novel isoflavone in vivo. High PPAR gamma agonism by compound **9** was thought to be one of the factors that may have led to the reduced blood glucose content of the drug treated ZDF rats. The alleviated body weight gain of the drug treated obese pre-diabetic rats elucidated due to favourable PPAR alpha and delta potency of compound **9** as discussed previously, was also envisaged to be responsible for the observed ameliorated blood glucose levels. The obtained results from the in vivo study of the novel pan PPAR compound **9** compared to the recent study of Keil et al.,[51] clearly highlighted the importance of pan PPAR agonist activity in effective treatment of diabetes. The novel dual PPAR gamma and delta sulfonylthiadiazole derivative reported by Keil et al.,[51] although was quite potent, but it was not able to address the weight gain adverse effect associated with the diabetes.

T2DM and obesity have been associated with fatty liver disease, characterized by enlarged liver size due to fat accumulation.[52,53] In week 6 of the study the rats were euthanized and their livers collected. The obese animals (ZDF), as expected, showed a higher liver mass than the lean controls (ZL). However, the drug treated ZDF rats exhibited a lower liver mass then the untreated ZDF rats (Table 4). The attenuated liver mass in the drug treated animals was envisaged to be due to PPAR alpha and delta agonistic efficacy (lipid lowering property) of the novel isoflavone. The acquired favourable data further enforced the vital complementary role of PPAR delta and alpha activation in improved treatment of T2DM and metabolic syndrome. In conclusion the obtained results clearly elucidated the in vivo activity of novel isoflavone **9** in improving in vivo model of pre-diabetes.

Table 4
The obtained liver mass of the four animal groups studied

Animal groups	Liver mass (g, mean)	
Group 1 (ZDF, drug treated)	19.7	(p <0.05)
Group 3 (ZDF, control)	23.9	
Group 2 (ZL, drug treated)	8.3	(p <0.05)
Group 4 (ZL, control)	8.6	

3. Conclusion

Twenty three dual PPARα and γ agonists were examined for pan PPAR activity by investigating their effects on PPARδ. The isoflavones induced the highest pan PPAR agonist activity within the three classes of compounds studied. Compounds **6**, **7**, **8**, and **9** were identified as the most efficacious pan PPARα, γ and δ agonists with PPARδ EC_{50} of 17.17, 22.34, 24.39, and 12.44 μM, respectively. These active compounds were at least twice as potent in activating PPARδ than the positive control bezafibrate (EC_{50} = 35.74 μM). Compound **9** with an EC_{50} of 12.44 μM induced the greatest PPARδ activation.

In summary, we have identified novel pan PPAR isoflavones **6**, **7**, **8**, and **9**, which may be more effective than the dual PPARα and γ agonists due to the beneficial effects of PPARδ activation (e.g. reduced cardiovascular complications, alleviation of weight gain, as well as, regulating effect on dyslipidemia). Such pan PPAR agonists may have an improved insulin sensitivity and glucose lowering effect than rosiglitazone due to higher PPARγ transactivation efficacy, and may also have reduced adverse effects due to the complementary beneficial effects of PPARα and PPARδ activation. In addition, as these drugs could target both hyperglycemia and dyslipidemia, they may be beneficial in targeting metabolic syndrome. Bezafibrate is the only pan PPAR agonist that is currently available, having been in clinical use as a lipid lowering drug for more than 25 years. Its role in metabolic syndrome has, however been studied only recently. The novel pan PPAR isoflavones **6**, **7**, **8**, and **9** may thus be promising drug candidates to be studied further as potential drugs for treatment of T2DM and metabolic syndrome.

4. Experimental

4.1. Cell culture

HEK293 cell line was obtained from American Type Culture Collection (ATCC, USA). All materials used for tissue culture were purchased from Invitrogen, Australia, unless specified. HEK293 cells were grown in Dulbecco's Modified Eagle's Medium/F-12 (DMEM/F-12) containing L-glutamine supplemented with penicillin (100 U/mL), streptomycin (100 μg/mL) and 10% (v/v) heat-inactivated fetal bovine serum.

4.2. PPARδ transfection and luciferase assay

The PPARδ transfection and luciferase procedures were performed as described previously by Bramlett et al.[36] with slight modifications. The HEK293 cell line was transfected with (1 μg/μL) tk-PPREx4-Luc plasmid (a kind gift from Dr Teruo Kawada, Kyoto University, Japan) plus (1 μg/μL) pBI-G-hPPARδ plasmid (a kind gift from Dr Sarah Roberts-Thomson, Queensland University, Australia) and (0.5 μg/μL) pSV-β-galactosidase (Promega, Australia) control plasmid. Cells were transfected with FuGENE 6 transfection reagent (Roche, Australia) in accordance with the manufacturer's instructions. After 24 h at 37 °C, cells were harvested and plated into 96-well plates (5×10^4 cells/well) in DMEM/F-12 media containing 10% FBS. The cells were allowed to attach overnight at 37 °C, after which they were treated with either the test drug samples (25 and 40 μM or bezafibrate (25 and 40 μM as PPARδ positive control or DMSO (0.1%) as vehicle control. The cells were lysed after 48 h incubation at 37 °C and assayed for luciferase and β-galactosidase activities using the Bright-Glo luciferase assay system and

Beta-Glo assay system (Promega, Australia), respectively, in accordance with the manufacturer's instructions. The results are expressed as relative luciferase activity normalized to the β-galactosidase signal (fold difference compared to vehicle control).

4.3. Cell proliferation assay

HEK293 cells were grown overnight in complete DMEM/F-12 media in 96-well plates (5×10^4 cells/well). The cells were then treated with varying concentrations of bezafibrate or isoflavones **6**, **7**, **8**, **9** (0–100 μM) or DMSO (0.1%). The treated cells were incubated for 48 h at 37 °C in a humidified atmosphere with 5% CO_2. MTS (tetrazolium salt) reagent (CellTiter96® Aqueous One Solution Cell Proliferation Assay, Promega) was then added followed by incubation for an additional 2 h at 37 °C and the absorbance was analyzed using a BMG POLARstar Galaxy Microplate Reader (λ: 490 nm). Interference from the background colour of each of the evaluated drugs was also measured in the same manner (λ: 490 nm) using a control 96-well plate without HEK293 cells. The colour control background absorbance readings were subtracted from the corresponding absorbance of the drug-treated cell containing wells to eliminate any colour interference. The cell proliferation results are expressed as % relative cell viability compared to DMSO vehicle control.

4.4. Statistical analysis

Statistical significance was assessed using the Student's unpaired two-tailed *t*-test within the GraphPad PRISM 5.02 software. *p*-Values less than 0.05 (p <0.05) were considered statistically significant.

4.5. Molecular modeling protocols

All the molecular modeling within this study was performed using Maestro software v9.1 (Schrödinger)[41] operating in a Linux environment.

4.5.1. Database preparation

Compounds **6**, **7**, **8**, **9**, rosiglitazone, MRL20, nTZDpa, GW409544 and 1FA were built and adjusted for chemical correctness using Maestro Build panel. Geometry minimizations were performed on all ligands using the OPLS_2005 force field[41] and the Truncated Newton Conjugate Gradient (TNCG).[41]

4.5.2. Preparing protein structures

The 2Q59 (resolution: 2.2 Å), 1K7L (resolution: 2.5 Å), 2Q5G (resolution: 2.7 Å), IFM6 (resolution: 2.1 Å), 2Q5S (resolution: 2.0 Å) and 2Q5P (resolution: 2.3 Å) crystal structures were downloaded from RCSB Protein Data Bank (http://www.pdb.org). Each of the crystal structures was then individually subjected to the protein preparation and refinement protocols using, Protein Preparation Wizard of the Maestro program. Briefly, the protein crystal structures were corrected for bond orders, hydrogen atoms and converting selenomethionines to methionines. The missing side chains and loops were predicted, the water molecules deleted beyond 5 Å of hetero groups, the appropriate protein chains and co-crystallized ligand selected and the state penalties calculated for the native ligand. The lowest obtained state value closest to 0.00 kcal/mol employed and the proteins further refined for H-bond assignment. The hydrogen bond network was optimized and ultimately the protein structures minimized using OPLS2005 force field. The acquired refined and minimized protein structures were then used individually in the grid generation and the docking process.

4.5.3. Ligand docking and post docking evaluation

Docking was performed using the Glide application of the Maestro program, with extra precision (XP) function to estimate protein-ligand binding affinities. Ligands were docked into the LBD of the prepared PPAR crystal structures. The acquired pose viewer file from the docking calculation was inspected using the XP Visualizer. The hydrogen bond network formed within 2.5 Å vicinity of each docked ligand and the receptor was examined with the default minimum donor angel of 120° and minimum acceptor angle of 90°.

4.6. In vivo protocols

Seven male pre-diabetic Zucker diabetic fatty (ZDF) rats and seven Zucker lean (ZL) rats, 9 weeks old, were purchased from Monash University Animal Services, Melbourne, Victoria. The animals were housed in groups of 3–4 per cage and accommodated at Sydney University, Animal House. They were studied for 6 weeks. The animals were divided into four groups: Group 1 (ZDF) and group 2 (ZL) were treated in the evenings with 3 mg/kg/day of potential diabetic drug, isoflavone 46 (prepared in acacia solution, Sigma), while group 3 (ZDF) and 4 (ZL) were exposed only to the acacia solution (controls). The animals were fed with standard pelleted diet (Animal House) and water. The amount of body weight gain monitored every evening prior to gavage drug treatment, while the amount of food intake measured every morning.

In week 5 of the study the animals were fasted overnight (~12 h), part of their leg was shaved (back of the leg) to allow better visualization of their main vein and a blood sample drawn from their leg. They were subsequently given orally 2 g/kg glucose solution (Sigma) and more blood samples collected at 15, 30, 45, 60, 90 and 120 min after the oral glucose intake. The blood glucose levels were quantified using a normal glucometer.

In week six, the rats were fasted overnight and put unconscious using a mixture of anaesthetic drugs, ketamine (75 mg/kg, Sigma) and xylazine (10 mg/kg, Sigma). The drugs were administered by an injection. When animals were under full anaesthesia, 1 ml blood sample was drawn from their heart using a 22 G needle positioned in a 30° angle under the middle of their ribs. The animals were then dissected and the following tissues collected: (1) adipose tissue located below the intestine, (2) skeletal muscle from back of the legs, (3) pancreas, (4) liver, (5) kidney and (6) small intestine. The mass of the obtained livers were measured and recorded.

4.7. Statistical analysis

Statistical significance was assessed using the Student's unpaired two-tailed *t*-test within the GraphPad PRISM 5.02 software. *p*-Values less than 0.05 (<0.05) were considered statistically significant.

Acknowledgments

We would like to thank Australian Research Council for funding. A.M. was supported by an Australian Postgraduate Award.

References and notes

1. Zoete, V.; Grosdidier, A.; Michielin, O. *Biochim. Biophys. Acta* **2007**, *1771*, 915.
2. Wang, N.; Ruiying, Y.; Liu, Y.; Mao, G.; Xi, F. *Circ. J.* **2011**, *75*, 528.
3. Di-Paola, R.; Esposito, E.; Mazzon, E.; Paterniti, I.; Galuppo, M.; Cuzzocrea, S. *J. Leukoc. Biol.* **2010**, *88*, 291.
4. Rubenstrunk, A.; Hanf, R.; Hum, D. W.; Fruchart, J. C.; Staels, B. *Biochim. Biophys. Acta* **2007**, 1065.
5. Willson, T. M.; Brown, P. J.; Sternbach, D. D. *J. Med. Chem.* **2000**, *43*, 527.
6. Desvergne, B.; Wahli, W. *Endocr. Rev.* **1999**, *20*, 649.
7. Belvisi, M. G.; Hele, D. J. *Chest* **2008**, *134*, 152.
8. Henke, B. R. *Prog. Med. Chem.* **2004**, *42*, 1.

9. Oliver, W. R.; Shenk, J. L.; Snaith, M. R. *Proc. Natl. Acad. Sci. U.S.A.* **2001**, *98*, 5306.
10. Chawla, A.; Lee, C. H.; Barak, Y. *Proc. Natl. Acad. Sci. U.S.A.* **2003**, *100*, 1268.
11. Cho, N.; Momose, Y. *Curr. Top. Med. Chem.* **2008**, *8*, 1483.
12. Pourcet, B.; Fruchart, J.; Staels, B.; Glineur, C. *Expert Opin. Emerg. Drugs* **2006**, *11*, 379.
13. Chang, F.; Jaber, L. A.; Berlie, H. D.; O'Connell, M. B. *Ann. Pharmacother.* **2007**, *41*, 973.
14. Calkin, A. C.; Thomas, M. C.; Cooper, M. E. *Curr. Opin. Investig. Drugs* **2003**, *4*, 444.
15. Tenenbaum, A.; Motro, M.; Fisman, E. Z. *Cardiovasc. Diabetol.* **2005**, 4. http://dx.doi.org/10.1186/1475-2840-4-14 [Online].
16. Chiarelli, F.; Di-Marzio, D. *Vasc. Health Risk Manage.* **2008**, *4*, 297.
17. Ahmed, I.; Furlong, K.; Flood, J.; Treat, V. P.; Goldstein, B. J. *Am. J. Ther.* **2007**, *14*, 49.
18. Blazer-Yost, B. L. *PPAR Res.* **2010**, Article ID 785369 [Online].
19. Bassaganya-Riera, J.; Guri, A. J.; Hontecillas, R. *J. Obesity* **2011**, Article ID 897894 [Online].
20. Zuo, Y.; Yang, H. C.; Potthoff, S. A.; Najafian, B.; Kon, V.; Ma, L. J.; Fogo, A. B. *Nephrol. Dial. Transpl.* **2012**, *27*, 174.
21. Friedland, S. N.; Leong, A.; Filion, K. B.; Genest, J.; Lega, I. C.; Mottillo, S.; Poirier, P.; Reoch, J.; Eisenberg, M. J. *Am. J. Med.* **2012**, *125*, 126.
22. Soskic, S. S.; Dobutovic, B. D.; Sudar, E. M.; Obradovic, M. M.; Nikolic, D. M.; Zaric, B. L.; Stojanovic, S.; Stokic, E. J.; Mikhailidis, D. P.; Isenovic, E. R. *Angiology* **2011**, *62*, 523.
23. Sharma, R. *J. Clin. Diagnostic Res.* **2008**, *2*, 659.
24. Balakumar, P.; Rose, M.; Ganti, S. S.; Krishan, P.; Singh, M. *Pharmacol. Res.* **2007**, *56*, 91.
25. Rosenson, R. S. *Am. J. Cardiol.* **2007**, *99*, 96B.
26. Azhar, S. *Future Cardiol.* **2010**, *6*, 657.
27. Gross, B.; Staels, B. *Best Pract. Res. Clin. Endocrinol. Metab.* **2007**, *21*, 687.
28. Stunes, A. K.; Westbroek, I.; Fossmark, R.; Berge, R. K.; Reseland, J. E.; Syversen, U. *PPAR Res.* **2011**, Article ID 436358 [Online].
29. Pirat, C.; Farce, A.; Lebègue, N.; Renault, N.; Furman, C.; Millet, R.; Yous, S.; Speca, S.; Berthelot, P.; Desreumaux, P.; Chavatte, P. *J. Med. Chem.* **2012**. http://dx.doi.org/10.1021/jm101360s [Online early access].
30. Yatsuga, S.; Suomalainen, A. *Hum. Mol. Genet.* **2012**, *21*, 526.
31. Adeghate, E.; Adem, A.; Hasan, M. Y.; Tekes, K.; Kalasz, H. *Open Med. Chem. J.* **2011**, *5*, 93.
32. Javiya, V. A.; Patel, J. A. *Indian J. Pharmacol.* **2006**, *38*, 243.
33. Ramachandran, U.; Kumar, R.; Mittal, A. *Mini-Rev. Med. Chem.* **2006**, *6*, 563.
34. Heald, M.; Cawthorne, M. A. *Handb. Exp. Pharmacol.* **2011**, *203*, 35.
35. Matin, A.; Gavande, N.; Kim, M. S.; Yang, N. X.; Salam, N. K.; Hanrahan, J. R.; Roubin, R. H.; Hibbs, D. E. *J. Med. Chem.* **2009**, *52*, 6835.
36. Bramlett, K. S.; Houck, K. A.; Borchert, K. M.; Dowless, M. S.; Kulanthaivel, P.; Zhang, Y.; Beyer, T. P.; Schmidt, R.; Thomas, J. S.; Michael, L. F.; Barr, R.; Montrose, C.; Eacho, P. I.; Cao, G.; Burris, T. P. *J. Pharmacol. Exp. Ther.* **2003**, *307*, 291.
37. Dang, Z. C.; Lowik, C. *J. Bone Miner. Res.* **2004**, *19*, 853.
38. Malapaka, R. R. V.; Khoo, S.; Zhang, J.; Choi, J. H.; Zhou, X. E.; Xu, Y.; Gong, Y.; Li, J.; Yong, E. L.; Chalmers, M. J.; Chang, L.; Resau, J. H.; Griffin, P. R.; Chen, Y. E.; Xu, H. E. *J. Biol. Chem.* **2012**, *287*, 183. http://dx.doi.org/10.1074/jbc.M111.29478.
39. Maiguma, T.; Fujisaki, K.; Itoh, Y.; Makino, K.; Teshima, D.; Takahashi-Yanaga, F.; Sasaguri, T.; Oishi, R. *N-S. Arch. Pharmacol.* **2003**, *367*, 289.
40. Zhao, Y.; Okuyama, M.; Hashimoto, H.; Tagawa, Y.; Jomori, T.; Yang, B. *Toxicol. In Vitro* **2010**, *24*, 154.
41. *Maestro, v9.1*; Schrödinger, LLC, New York, NY, 2011.
42. Gampe, R. T.; Montana, V. G.; Lambert, M. H.; Miller, A. B.; Bledsoe, R. K.; Milburn, M. V.; Kliewer, S. A.; Willson, T. M.; Xu, H. E. *Mol. Cell* **2000**, *5*, 545.
43. Bruning, J. B.; Chalmers, M. J.; Prasad, S.; Busby, S. A.; Kamenecka, T. M.; He, Y.; Nettles, K. W.; Griffin, P. R. *Structure* **2007**, *15*, 1258.
44. Xu, H. E.; Lambert, M. H.; Montana, V. G.; Plunket, K. D.; Moore, L. B.; Collins, J. L.; Oplinger, J. A.; Kliewer, S. A.; Gampe, R. T.; McKee, D. D.; Moore, J. T.; Willson, T. M. *Proc. Natl. Acad. Sci.* **2001**, *98*, 13919.
45. Pettersson, I.; Ebdrup, S.; Havranek, M.; Pihera, P.; Korinek, M.; Mogensen, J. P.; Jeppesen, C. B.; Johanssona, E.; Sauerberg, P. *Bioorg. Med. Chem. Lett.* **2007**, *17*, 4625.
46. Augstein, P.; Salzsieder, E. *Methods Mol. Biol.* **2009**, 159–189.
47. Khaodhiar, L.; Cummings, S.; Apovian, C. M. *Curr. Diabetes Rep.* **2009**, *9*, 348–354.
48. Islam, A., Akhtar, A.; Islam-Khan, R.; Hossain, S.; Khurshid-Alam, M.; Wahed, M. I. I.; Amran, S.; Rahman, B. M.; Ahmed, M. *Pakistan J. Pharm. Sci.* **2009**, *22*, 402–404.
49. *Glucose Tolerance Test. Medline Plus*; U.S. National Library of Medicine, National Institutes of Health (NIH).
50. Augstein, P.; Salzsieder, E. *Methods Mol. Biol.* **2009**, *560*, 159.
51. Keil, S.; Matter, H.; Schçnafinger, K.; Glien, M.; Mathieu, M.; Marquette, J. P.; Michot, N.; Haag-Diergarten, S.; Urmann, M.; Wendler, W. *ChemMedChem* **2011**, *6*, 633–653.
52. Akbar, D. H.; Kawther, A. H. *Diabetes Care* **2003**, *26*, 3351.
53. Wu, C. H.; Lin, M. C.; Wang, H. C.; Yang, M. Y.; Jou, M. J.; Wang, C. J. *J. Food Sci.* **2011**, *76*, T65.